Supplemental Material can be found at:
http://www.jlr.org/content/suppl/2005/03/17/M400428-JLR200.DC1.html

Retina expresses microsomal triglyceride transfer protein: implications for age-related maculopathy[S]

Chuan-Ming Li,* J. Brett Presley,* Xueming Zhang,* Nassrin Dashti,† Byong Hong Chung,† Nancy E. Medeiros,§ Clyde Guidry,* and Christine A. Curcio[1,*]

Department of Ophthalmology* and Division of Gerontology and Atherosclerosis Research Program,† Department of Medicine, University of Alabama School of Medicine, Birmingham, AL; and Retina Specialists of North Alabama,§ Huntsville, AL

Abstract The principal extracellular lesions of age-related maculopathy (ARM), the leading cause of vision loss in the elderly, involve Bruch's membrane (BrM), a thin vascular intima between the retinal pigment epithelium (RPE) and its blood supply. With age, 80–100 nm solid particles containing esterified cholesterol (EC) accumulate in normal BrM, and apolipoprotein B (apoB) immunoreactivity is detectable in BrM- and ARM-associated lesions. Yet little evidence indicates that increased plasma cholesterol is a risk factor for ARM. To determine if RPE is capable of assembling its own apoB-containing lipoprotein, we examined RPE for the expression of microsomal triglyceride transfer protein (MTP), which is required for this process. Consistent with previous evidence for apoB expression, MTP is expressed in RPE, the ARPE-19 cell line, and, unexpectedly, retinal ganglion cells, which are neurons of the central nervous system. De novo synthesis and secretion of neutral lipid by ARPE-19 was supported by high levels of radiolabeled EC and triglyceride in medium after supplementation with oleate. Lipoprotein assembly and secretion is implicated as a constitutive retinal function and a plausible candidate mechanism involved in forming extracellular cholesterol-containing lesions in ARM. The pigmentary retinopathy and neuropathy of abetalipoproteinemia (Mendelian Inheritance of Man 200100; Bassen-Kornzwieg disease), which is caused by mutations in the *MTP* gene, may involve loss of function at the retina.—Li, C-M., J. B. Presley, X. Zhang, N. Dashti, B. H. Chung, N. E. Medeiros, C. Guidry, and C. A. Curcio. **Retina expresses microsomal triglyceride transfer protein: implications for age-related maculopathy. *J. Lipid Res.* 2005.** 46: **628–640.**

Supplementary key words lipoprotein assembly • esterified cholesterol • retinal pigment epithelium • Bruch's membrane • abetalipoproteinemia

Embryologically part of the central nervous system, the retina (**Fig. 1A**) converts light energy to electrochemical signals for transmission to the brain. The photoreceptors are supported by the retinal pigment epithelium (RPE), a monolayer with diverse functions including daily phagocytosis of the distal tips of photoreceptor outer segments (OS), and the choroid, a vascular bed with the body's highest blood flow. The choriocapillaris is a dense capillary plexus in the innermost choroid, and Bruch's membrane (BrM) is a thin vascular intima between the RPE and the choriocapillaris (Fig. 1B, arrowheads). In human retina, the macula subserves high-acuity vision and is vulnerable to age-related maculopathy (ARM), the major cause of vision loss among the elderly of industrialized societies. The most prominent histopathologic and clinical signs of ARM are extracellular lesions [drusen (Fig. 1E, F) and basal linear deposits (not shown)] in the RPE/BrM complex that ultimately impact vision by the photoreceptors (1, 2). Choroidal neovascularization, an invasion of choriocapillaries across BrM and lateral spread within the plane of drusen and basal linear deposit (see 3), is the principal sight-threatening complication of ARM's obscure underlying degeneration.

Recent findings highlight a role for lipids and lipoproteins in this degeneration. These include a protective effect of the apolipoprotein E4 (apoE4) genotype in populations and the presence of apoB and apoE and histochemically identified lipids in aging- and ARM-associated drusen and deposits in human tissues (4–8) (Fig. 1E, F). The best established risk factor for early ARM is advanced age (9). A

Manuscript received 28 October 2004 and in revised form 23 December 2004.

Published, JLR Papers in Press, January 16, 2005.
DOI 10.1194/jlr.M400428-JLR200

Abbreviations: ABL, abetalipoproteinemia; apoB, apolipoprotein B; apoBEC-1, apolipoprotein B-editing complex-1; ARM, age-related maculopathy; BrM, Bruch's membrane; EC, esterified cholesterol; ESI/MS, electrospray ionization mass spectrometry; INL, inner nuclear layer; MCT3, monocarboxylate transporter 3; MTP, microsomal triglyceride transfer protein; OS, outer segments of photoreceptors; RGC, retinal ganglion cell; RPE, retinal pigment epithelium; TC, total cholesterol; TG, triglyceride; UC, unesterified cholesterol.

[1] To whom correspondence should be addressed.
e-mail: curcio@uab.edu

[S] The online version of this article (available at http://www.jlr.org) contains an additional table.

Copyright © 2005 by the American Society for Biochemistry and Molecular Biology, Inc.

This article is available online at http://www.jlr.org

Downloaded from www.jlr.org by guest, on June 14, 2012

Supplemental Material can be found at:
http://www.jlr.org/content/suppl/2005/03/17/M400428-JLR200.DC1.html

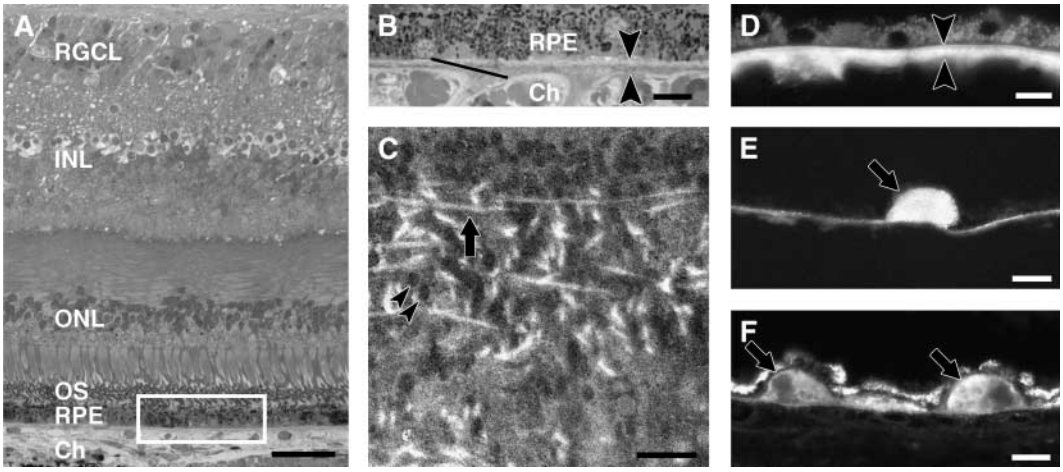

Fig. 1. Esterified cholesterol (EC), apolipoproteins, and lipoprotein-like particles in macular Bruch's membrane (BrM) of aged human eye. A: A 1 μm thick toluidine blue-stained section of macular retina. Ch, choroid; INL, inner nuclear layer; ONL, outer nuclear layer (nuclei of photoreceptors); os, photoreceptor outer segments; RGCL, retinal ganglion cell layer; RPE, retinal pigment epithelium. The box delimits the area shown in B and D. Bar = 50 μm. B: A 1 μm thick section showing RPE, BrM (between arrowheads), and choroid (Ch). The line shows the plane of the section in C. Bar = 10 μm. C: Electron micrograph of BrM postfixed in osmium tannic acid paraphenylenediamine shows lipoprotein-like particles (arrowheads) among collagen fibrils (arrow) (12). Bar = 1 μm. D: Cryosection (10 μm thick) showing RPE autofluorescence and filipin fluorescence caused by EC (12) in BrM (between arrowheads). Bar = 10 μm. E: Drusen containing EC (arrow). Bar = 20 μm. F: Drusen containing apolipoprotein B (apoB) immunoreactivity (arrows). Bar = 20 μm.

large age-related change in normal human retina is the accumulation of neutral lipids in BrM throughout adulthood (7, 10–13). This material binds oil red O and contains esterified cholesterol (EC) (Fig. 1D) and triglyceride (TG) (7, 10–12). Furthermore, EC is associated with 80–100 nm diameter solid particles (Fig. 1C) that have surface and core substructure (12–14). Understanding the pathway(s) that lead to neutral lipid deposition in normal human BrM is critical for understanding the pathway(s) that lead to drusen and basal linear deposits in ARM. Studies of BrM lipid composition (11, 12, 15) implicate extravasation of plasma lipoproteins from the choroid or deposition from intraocular cells as candidate mechanisms. The RPE processes abundant lipids from ingested OS membranes (16). It synthesizes and secretes BrM constituents (17, 18) and contains biosynthetic machinery for numerous druse-associated proteins (19, 20), including apoE (6, 21). However, a mechanism to account for the abundant EC and other neutral lipids in normal BrM is unknown.

Atherosclerotic cardiovascular disease and ARM feature apoB- and cholesterol-containing extracellular lesions in a vascular intima and shared risk factors of smoking and hypertension (22, 23), among others. However, only 1 epidemiologic study of 23 since 1963 (24) links ARM with increased total plasma cholesterol (see supplementary table), a defining risk factor for atherosclerosis (25). Although not the strongest indicator of cardiovascular risk, total plasma cholesterol was the one measure common to all of these investigations. Many studies were small and used different ARM end points. However, if plasma lipoproteins were the major source of cholesterol in BrM and sub-RPE deposits, then a more consistent association should have been detected despite these limitations. This paradox could be reconciled if an apoB-containing lipoprotein of intraocular origin were the major source of early-arriving EC in BrM- and ARM-associated lesions, in contrast to apoB-containing lipoprotein from plasma that arrives early in incipient atherosclerotic plaques (26, 27). This idea is credible, because native human RPE contains apoB mRNA and protein (8, 19), and the thermal behavior of birefringent EC crystals in BrM differs from that in sclera, which accumulates EC from plasma apoB-containing lipoprotein (28).

If the RPE synthesizes, assembles, and secretes an apoB-containing lipoprotein with a neutral lipid core, it should also express microsomal triglyceride transfer protein (MTP). This soluble heterodimer in the endoplasmic reticulum lumen is required for apoB-containing lipoprotein assembly (29, 30). Cells expressing apoB without MTP cannot secrete lipoproteins, and all cells expressing MTP also secrete apoB-containing lipoprotein (31–34). *MTP* mutations resulting in a lack of functional protein cause abetalipoproteinemia (ABL; MIM 200100, Bassen-Kornzwieg disease), a rare autosomal recessive disorder. ABL features the absence of plasma apoB-containing lipoprotein, fat malabsorption, steatorrhea, acanthocytosis, ataxic neuropathy, and, importantly, a pigmentary retinopathy (31, 35). To begin evaluating our hypothesis, we determined whether MTP was present in human neurosensory retina, native RPE, and ARPE-19, a spontaneously arising transformed cell line with differentiated properties (36–38). We then determined that ARPE-19 could secrete EC-containing particles, confirming these results in primary porcine RPE. Of a lipoprotein's surface and core compo-

Downloaded from www.jlr.org by guest, on June 14, 2012

Supplemental Material can be found at:
http://www.jlr.org/content/suppl/2005/03/17/M400428-JLR200.DC1.html

nents, we focused on EC, because it is localized exclusively within BrM (Fig. 1D). Our results have implications for ARM pathobiology, retinal cell biology, and ABL.

MATERIALS AND METHODS

Human tissue

Human donor eyes with grossly normal maculas were obtained from the Alabama Eye Bank within 6 h of death (n = 8, 65–85 years for RT-PCR; n = 9, 30–92 years for Western blot; n = 9, 38–89 years for immunohistochemistry). For immunohistochemistry, anterior segments of donor globes were removed by encircling cuts at the corneoscleral limbus. Posterior segments were immersed in 4% paraformaldehyde in 0.1 M phosphate buffer for 6–16 h and stored in 1% paraformaldehyde at 4°C until used. To isolate retinal mRNA and protein, globes were incised at the equator, and anterior segments were removed with vitreous body attached. Small forceps were used to peel the retina from the RPE/choroid while the scleral eyecup was stabilized with another forceps.

Cell culture

ARPE-19 and HepG2 cell lines were obtained from the American Type Culture Collection at passage 22 and subjected to RT-PCR, Western blot, and secretion experiments after 2 passages. ARPE-19 cells were also provided by Dr. N. J. Philp (Thomas Jefferson University) (37). For RT-PCR and Western blot, cells were plated in T-75 flasks or on six-well plates and grown for 4 weeks in DMEM/F12 (1:1) supplemented with 10% fetal calf serum as described (36). Medium was changed twice weekly. HepG2 cells were grown on six-well plates in MEM containing 10% fetal calf serum for 5 days with a medium change every other day. Primary cultures of porcine RPE were prepared as described (39) and used 24 h after isolation.

RT-PCR and sequencing

Total RNA was isolated from human retina, RPE, ARPE-19 cells, and HepG2 cells as described (8). Total RNA from porcine retina, RPE, and liver was isolated with Trizol Reagent (Invitrogen, Carlsbad, CA). Human ileum mRNA was purchased from Stratagene. Primers used for RT-PCR are listed in **Table 1**. To distinguish between amplified mRNA and genomic DNA, primers were designed to span intron boundaries except where noted. One-step RT-PCR was used for human apoB and porcine apoB and MTP, as described (8). Two-step RT-PCR was used for others. The first-strand cDNA was synthesized with Omniscript™ Reverse Transcriptase (Qiagen, Valencia, CA). The PCR Core System (Promega, Madison, WI) was used for PCR. The cDNA was denatured for 4 min at 94°C before cycling. The reaction was amplified through 35 cycles of 45 s at 94°C (denaturing), 45 s at 55–66°C (annealing), and 1 min at 72°C (extension), then incubated for 10 min at 72°C. Cross-contamination of retinal and RPE mRNA was assessed by checking the expression of the retina-specific gene *RHO* in RPE mRNA and the RPE-specific gene *VMD2* in neurosensory retina mRNA. All results for neurosensory retina and RPE were obtained in at least one sample without contamination. The primers 5′-GAG AAA CTG ACT GCT CTC AC-3′ (sense) and 5′-ATG ATA GTG CTC ATC AAG ACT T-3′ (antisense) were used to amplify a 234 bp human apoB cDNA fragment containing the editing site of apoB-48. The cDNA sequence was analyzed as described (8).

Western blot

Protein extracts of human retina, RPE, ARPE-19 cells, and HepG2 cells were prepared and Western blot analysis was performed as described (8). Polyclonal rabbit anti-bovine MTP 97 kDa large subunit (40) was a gift from Dr. J. R. Wetterau at Bristol-Meyers-Squibb (used at 1:500). Monoclonal anti-human apoB [1D1, recognizing an N-terminal epitope between amino acids 474 and 539 (41)] was a gift from Dr. R. Milne at the University of Ottawa (used at 1:1,000). Secondary antibodies, horseradish peroxidase-conjugated donkey anti-rabbit IgG, and donkey anti-

TABLE 1. The sequences of PCR primers and expected fragment sizes

Species	Gene	Protein	Primers	Expected Size
				bp
Human	APOB	Apolipoprotein B	F: 5′-GAG GTC ATC AGG AAG GGC TCA AAG-3′ R: 5′- GGG ATC ACC TCC GTT TTG GTG GTA-3′	419
Human	APOB	Apolipoprotein B	F: 5′-GAG AAA CTG ACT GCT CTC AC-3′ R: 5′-ATG ATA GTG CTC ATC AAG ACT T-3′	234
Human	MTP	Microsomal triglyceride transfer protein (large polypeptide, 88 kDa)	F: 5′-GGA CTT TTT GGA TTT CAA AAG TGA C-3′ R: 5′-GGA GAA ACG GTC ATA ATT GTG-3′	698
Human	PDI	Protein disulfide isomerase	F: 5′-TGA CCT TTG GCC TCA CAG ACC-3′ R: 5′-TAC TTC TCA GCC AAT GCC TCC-3′	715
Human	APOBEC1	Apolipoprotein B mRNA-editing enzyme, catalytic polypeptide 1	F: 5′-ACA CCA CCA ATC ACG TGG AAG-3′ R: 5′-TCA TCT CCA AGC CAC AGA AGG-3′	542
Human	SOAT1	Sterol *O*-acyltransferase (acyl-CoA:cholesterol acyltransferase) 1	F: 5′-AAG TTG ACA GCA GAG GCA GA-3′ R: 5′-ATC CAC CAG GTC CAA ACA AC-3′	413
Human	SOAT2	Sterol *O*-acyltransferase (acyl-CoA:cholesterol acyltransferase) 2	F: 5′-GCT GCT GCT GGA GTT TGA CC-3′ R: 5′-AGC AGG CAT AGA GCA CAC ATC-3′	494
Porcine	APOB	Apolipoprotein B	F: 5′-TGG GAA CGA AGA TCA CAC CTA C-3′ R: 5′-GGG AAG CCA CAA AGT TCT TCA C-3′	351
Porcine	MTP	Microsomal triglyceride transfer protein	F: 5′-TGA CCT ACC AGG CTC ATC AA-3′ R: 5′-GGA TGG CCG TGT ACT TAG AA-3′	336

All primers for human genes were designed based on GenBank gene sequences. Primers for porcine MTP were from Lu et al. (79). ACAT1 and ACAT2 are gene aliases for SOAT1 and SOAT2. F, forward primer; R, reverse primer.

Downloaded from www.jlr.org by guest, on June 14, 2012

Supplemental Material can be found at:
http://www.jlr.org/content/suppl/2005/03/17/M400428-JLR200.DC1.html

mouse IgG were purchased from Jackson Immunoresearch (West Grove, PA; used at 1:2,000). Immunoblotted proteins were detected by enhanced chemiluminescence (Amersham Biosciences, Piscataway, NJ).

Immunohistochemistry

Cryosections of human retina and choroid were prepared as described (8). Except where noted, reagents were purchased from Vector Laboratories (Burlingame, CA). For localizing apoB, MTP, and monocarboxylate transporter 3 (MCT3) in human RPE, sections were bleached before staining as described (42). Briefly, cryosections were removed from −20°C, heated for 30 min at 50–55°C, and rinsed with PBS. Slides were incubated in 0.05% potassium permanganate for 25 min, rinsed for 5 min in distilled water, flooded with 35% peracetic acid in a humidified container for 15 min, and washed in distilled water for 10 min, all at room temperature. Next, sections were heated at 50–55°C for 30 min and incubated with the primary antibodies anti-apoB (Biodesign, Saco, ME; 1:500), anti-MTP (1:100), and anti-MCT3 (1:100; a gift from Dr. N. J. Philp) followed by biotinylated secondary antibodies, peroxidase-conjugated streptavidin, and the VIP Peroxidase Substrate Kit. Appropriate controls were processed with stained sections. For localizing apoB, MTP, and Brn3a in neurosensory retina, immunohistochemistry was performed as described (43). Briefly, sections were incubated overnight at 4°C with primary antibodies against apoB (1:1,000), MTP (1:100), and Brn3a (Chemicon, Temecula, CA; 1:100). Next, biotinylated secondary antibodies and the ABC-Peroxidase Kit or the ABC-Alkaline Phosphatase Kit were applied. Immunoreactivity was visualized with the VIP Peroxidase Substrate Kit for MTP and apoB and the Blue Alkaline Phosphatase Substrate Kit III for Brn3a. For double labeling, sections were incubated first with anti-Brn3a and alkaline phosphatase substrate, then with anti-apoB or MTP and VIP substrate. For apoB and MTP fluorescence double labeling, sections were incubated with biotinylated secondary antibody and allophycocyanin-conjugated streptavidin (eBioscience, San Diego, CA) for apoB (at 1:500) and FITC-conjugated goat anti-rabbit IgG (Jackson Immunoresearch) for MTP.

Extraction of lipids from cells and medium

Lipids were extracted from culture medium using chloroform-methanol-water (14:7:1) (44). Aliquots of organic phase were evaporated under nitrogen and solubilized in isopropanol. Lipids were extracted from PBS-washed cells on six-well plates using two 30 min incubations with 1.0 ml of hexane-isopropanol (3:2, v/v). Aliquots of pooled extracts were evaporated under nitrogen, solubilized in isopropanol, vortexed, and sonicated for 15 min. Remaining cellular material was digested in 0.1 N NaOH/0.1% SDS to determine protein content (DC Protein Assay Kit; Bio-Rad).

Enzymatic fluorimetric assay for total and unesterified cholesterol

Total cholesterol (TC) and unesterified cholesterol (UC) mass in extracts of native RPE and cultured cells was determined by enzymatic fluorimetric assay as described (12, 45). The resulting fluorescence was read at 325 nm excitation wavelength and 415 nm emission wavelength using a model F-2500 Fluorescence Spectrophotometer (Hitachi). The EC value was defined as the difference between the TC and UC values. UC solubilized in isopropanol was used as a standard.

Electrospray ionization mass spectrometry for cholesteryl esters

Evaporated 0.5 ml aliquots of extracts from cells and medium were solubilized in 50 μl of isopropanol, vortexed, and sonicated for 15 min. Lipids were separated by reversed-phase HPLC on a 10 cm × 2.1 mm inner diameter Aquapore C8 column at a flow rate of 0.2 ml/min using a linear 50–100% isopropanol gradient in 10 mM ammonium acetate. Positive ion mass spectra were recorded in the Ionspray™ mode, with an orifice potential of 50 V (API III triple quadrupole mass spectrometer; PE-Sciex, Concord, Ontario, Canada). Under these conditions, ammonium $(M+NH_4)^+$ adducts of cholesteryl esters were observed. External standards consisted of cholesteryl palmitate (16:0), cholesteryl linoleate (18:2), cholesteryl oleate (18:1), cholesteryl stearate (18:0), cholesteryl arachidonate (20:4), and cholesteryl docosahexanoate (22:6; ester of *cis*-4,7,10,13,16,19-docosahexanoic acid) dissolved in isopropanol at concentrations from 10 nM to 20 μM. The mass-to-charge ratios (molecular weight plus ammonium ion) for these compounds were 642, 666, 668, 670, 694, and 714, respectively. Standards were obtained from Sigma and Steraloids (for 22:6; Newport, RI). Concentrations were expressed as nanomoles per milliliter. Before extraction, β-sitosteryl acetate (mass-to-charge ratio, 474) was added to each sample as an internal standard (final concentration, 4.17 μM). The mean ester concentration for each sample was normalized to cholesteryl oleate.

Conditioned medium experiments

ARPE-19 cells were cultured on six-well dishes for 2 weeks. After cells were washed, 1 ml of DMEM/F12 containing 0.4 mM oleic acid and 1.5% FFA-free BSA, prepared as described (46), was added to each well. After 24 h of incubation, the medium was collected and centrifuged at 5,000 rpm for 5 min to remove cellular debris. The supernatant was withdrawn for lipid extraction and analysis of cholesterol mass and composition.

Metabolic labeling experiments

ARPE-19 cells were cultured for 2 weeks, maintenance medium was removed, and cells were washed twice with PBS. Serum-free DMEM containing 5 μCi/ml [^{3}H]oleate (5,000 dpm/nmol) bound to 1.5% FFA-free BSA was added. After 24 and 48 h, medium was collected and centrifuged at 5,000 rpm for 5 min to remove cellular debris, and the supernatant was withdrawn. Lipids were extracted from medium and PBS-washed cells (see above). Extracts were evaporated under nitrogen, solubilized in chloroform, and applied to LHPKD silica gel 60A TLC plates (Whatman). Plates were developed in petroleum ether-diethyl ether-acetic acid (84:15:1), sprayed with 3% copper acetate in 8% phosphoric acid solution, and heated to reveal bands. Chloroform-solubilized oleic acid, UC, cholesteryl oleate, triolein, and trilinolenin served as standards. Bands corresponding to EC, TG, and phospholipid were excised, and radioactivity was quantified by liquid scintillation counting. Blank areas between bands were counted as background. A band at the UC position was not reliably separated from diglycerides in this system. Results from two to three wells are reported for one experiment.

Density gradient ultracentrifugation and negative stain electron microscopy

ARPE-19 cells were cultured for 2–4 weeks in T-75 flasks. After cells were washed twice with PBS, 10 ml of serum-free DMEM/F12 containing 0.4 mM oleic acid bound to 1.5% BSA was added. After 24 h of incubation, conditioned medium was harvested and cellular debris was pelleted by centrifugation at 2,000 rpm for 20 min at 4°C. Density was adjusted to 1.24 g/ml (by weight) by adding solid KBr. Ten milliliters of sample was added to an SW41 centrifuge tube, overlaid with 2 ml of 1.21 g/ml KBr, and centrifuged at 40,000 rpm for 36 h at 10°C in a Beckman L80 ultracen-

Downloaded from www.jlr.org by guest, on June 14, 2012

Supplemental Material can be found at:
http://www.jlr.org/content/suppl/2005/03/17/M400428-JLR200.DC1.html

trifuge using an SW41Ti rotor. Supernatant (0.2 ml) was drawn from the tube top. Lipoprotein particles in the d ⩽ 1.21 g/ml fraction were visualized as described (47) with modifications. Samples were dialyzed overnight in 0.125 M ammonium acetate, 2.6 mM ammonium carbonate, and 0.26 mM tetrasodium EDTA (pH 7.4, 4°C) and then mixed with equal volumes of 2% potassium phosphotungstic acid. A droplet was placed in the center of a Formvar-coated copper grid freshly decharged in 100% ethanol and dried for 30 s. The droplet edge, with concentrated particles, was viewed on a JEOL 1200 electron microscope. Samples from the d ⩽ 1.21 g/ml fraction and medium of nonsupplemented cells were also examined.

RESULTS

Expression of apoB and MTP in human retina

To test the possibility that neurosensory retina (19), in addition to RPE (8), contains mRNA transcripts for apoB, we performed RT-PCR analysis of RNA obtained from neurosensory retina, native RPE, ARPE-19 cells, and human hepatoma HepG2 cells as a positive control. **Figure 2A** shows RT-PCR products consistent with the predicted 419 bp in all lanes. ApoB-100 and apoB-48 are products of the same gene, with apoB-48 arising from posttranscrip-

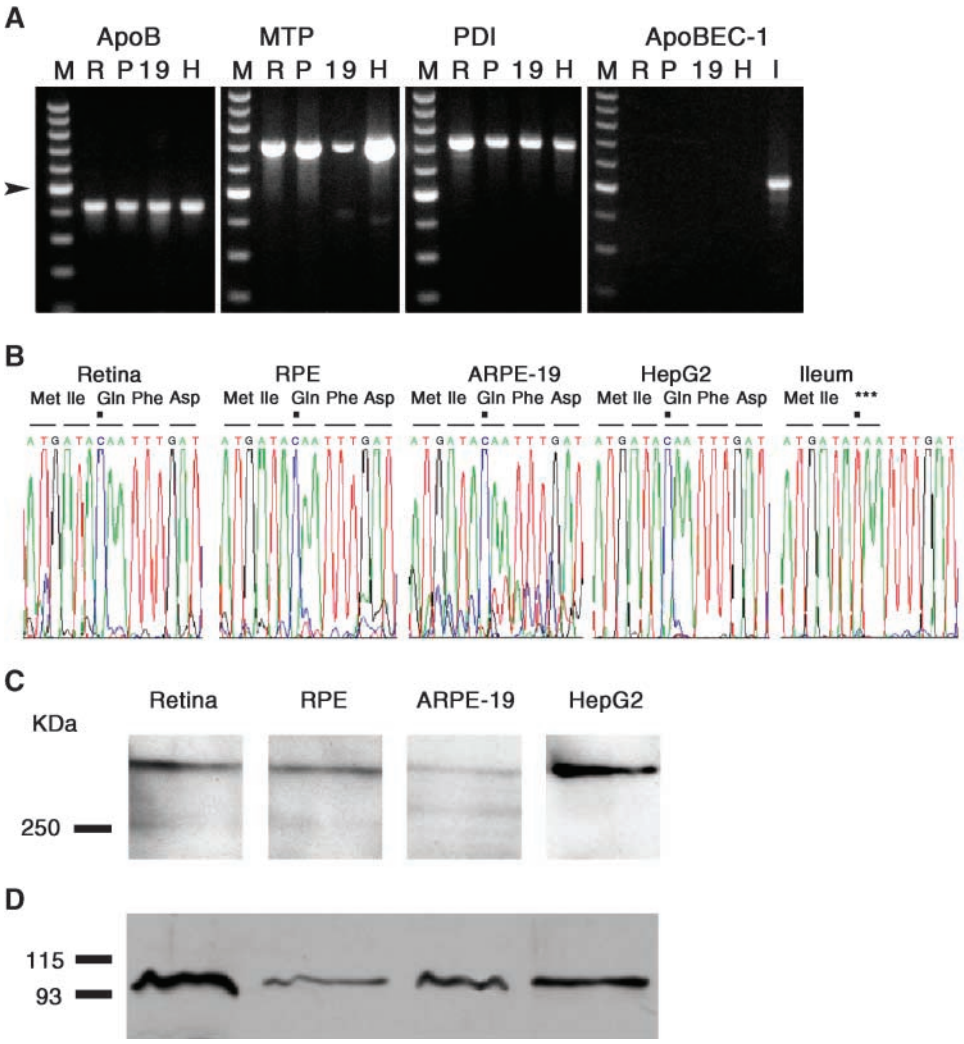

Fig. 2. ApoB-100 and microsomal triglyceride transfer protein (MTP) expression in human retina (R), RPE (P), ARPE-19 (19), and HepG2 (H) cells. A: RT-PCR analyses of apoB, MTP, protein disulfide isomerase (PDI), and apoB-editing complex-1 (apoBEC-1), as described in Materials and Methods. Expected lengths of RT-PCR products are listed in Table 1. ApoB, MTP, and protein disulfide isomerase were detected in retina, RPE, ARPE-19, and HepG2 cells. ApoBEC-1 was detected in ileum (I) only. M, 100 bp DNA ladder; arrowhead, 500 bp. B: Partial nucleic acid sequence and deduced amino acid sequence of apoB from different tissues and cells. RT-PCR fragments in retina, RPE, ARPE-19, and HepG2 contain a CAA codon, encoding Gln-2153 in apoB-100, and in ileum contain a TAA, the stop codon in apoB-48. Closed squares indicate the editing site of apoB-48. Asterisks indicate a stop codon present only in ileum mRNA. C: ApoB expression in retina and RPE. Western blotting was performed using detergent-extracted proteins from retina (120 μg), RPE (88 μg), ARPE-19 (71 μg), and HepG2 (41 μg) with mouse anti-human apoB. D: MTP expression in retina and RPE. Extracts of retina (100 μg), RPE (72 μg), ARPE-19 (119 μg), and HepG2 (43 μg) were subjected to Western blot with rabbit anti-bovine MTP 97 kDa large subunit. MTP was detected in all four samples. HRP-conjugated secondary antibody and chemiluminescence were used in C and D.

Downloaded from www.jlr.org by guest, on June 14, 2012

Supplemental Material can be found at:
http://www.jlr.org/content/suppl/2005/03/17/M400428-JLR200.DC1.html

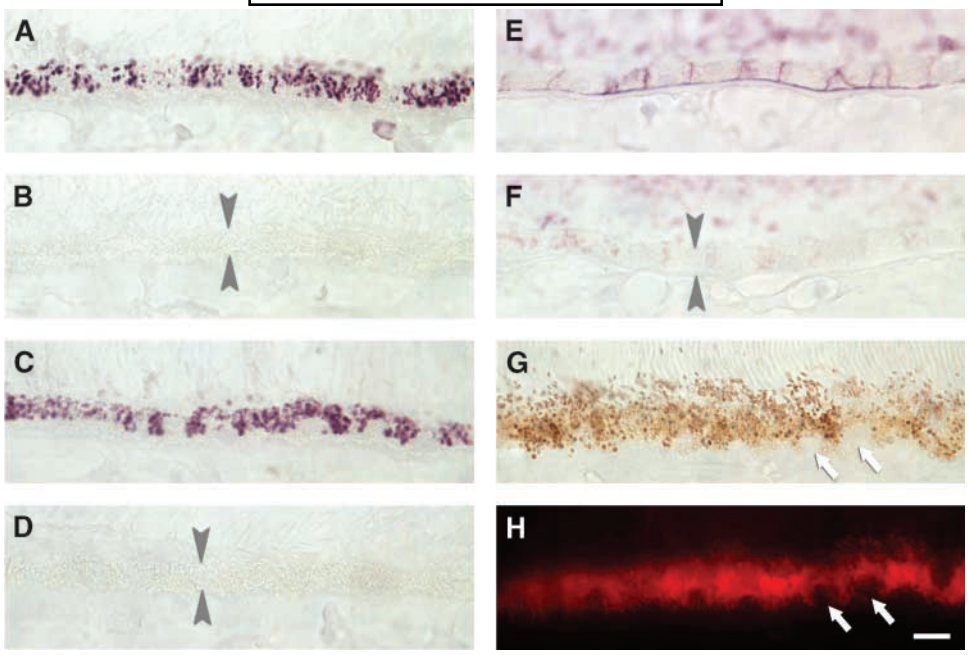

Fig. 3. ApoB and MTP immunoreactivity in bleached RPE of normal human macula. Immunoreactivity is purple. Arrowheads in B, D, and F delimit bleached RPE. Bar = 20 μm. A: Goat anti-human apoB labels clumps in RPE. B: No clumps are visible in a section treated with goat IgG. C: Rabbit anti-bovine MTP labels similar clumps in RPE. D: No clumps are visible in a section treated with rabbit IgG. E: The basolateral location of monocarboxylate transporter 3 is unaffected by bleach treatment. Label in outer segments (out of focus) is nonspecific. F: No basolateral labeling is apparent in a bleached section treated with rabbit IgG, but nonspecific outer segment labeling remains. G: Melanin granules in a section that was unbleached and unexposed to antibodies are smaller than apoB- and MTP-positive clumps. Arrows indicate the same cells in G and H. H: Autofluorescent lipofuscin granules in the same section as in G are smaller and more numerous than apoB- and MTP-positive clumps.

tional C-to-U substitution editing of apoB-100 mRNA by apoB-editing complex-1 (apoBEC-1) (48). To determine if apoB mRNA from human retina and RPE specifies apoB-100 or apoB-48, a 234 bp RT-PCR product containing the RNA-editing site was sequenced from both 5′ and 3′ ends. Sequencing revealed that apoB cDNA from human retina, RPE, ARPE-19 cells, and HepG2 cells contains a CAA codon, signifying apoB-100, and not a TAA stop codon, as in human ileum (Fig. 2B). Accordingly, we detected apoBEC-1 mRNA in ileum but not in retina, RPE, or HepG2 cells (Fig. 2A).

To test whether RPE and retina express mRNA for MTP, RT-PCR was performed using total RNA isolated from retina, RPE, ARPE-19 cells, and HepG2 cells as a positive control. RT-PCR products at the expected 698 bp size were generated in all lanes. In addition to transcripts for the 97 kDa large subunit MTP unit, all lanes showed transcripts at 715 bp for protein disulfide isomerase, the smaller subunit of the MTP heterodimer (Fig. 2A).

To determine if human retina and RPE express apoB and MTP proteins, detergent-extracted retina, RPE, ARPE-19, and HepG2 were subjected to SDS-PAGE and probed with a monoclonal antibody against human apoB (Fig. 2C) and a polyclonal antibody against bovine MTP 97 kDa large subunit (Fig. 2C, D). ApoB was detected in retina, RPE, ARPE-19, and HepG2, as indicated by bands at 512 kDa with faint bands at lower molecular masses. The large subunit of MTP was detected in all samples, indicated by prominent bands at 97 kDa (Fig. 2D).

Localization of apoB and MTP in human RPE

To localize apoB and MTP in highly pigmented native human RPE, we treated cryosections with potassium permanganate and peracetic acid to bleach melanin (49). ApoB and MTP immunoreactivity was detected in moderately sized clumps in RPE cell bodies (**Fig. 3A, C**, re-

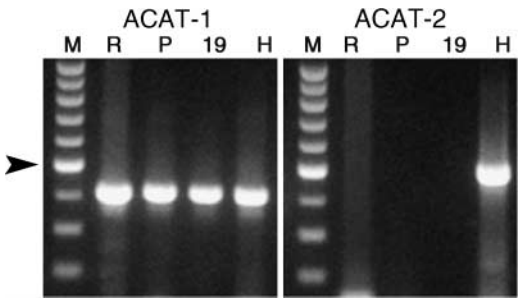

Fig. 4. Expression of ACAT genes in native human retina (R), RPE (P), ARPE-19 (19), and HepG2 (H) cells. Total RNA was isolated and RT-PCR was performed as described in Materials and Methods. Expected lengths of RT-PCR products are listed in Table 1. ACAT1 was detected in human retina, RPE, ARPE-19, and HepG2. ACAT-2 was detected in HepG2 only. M, 100 bp DNA ladder; arrowhead, 500 bp.

Downloaded from www.jlr.org by guest, on June 14, 2012

Supplemental Material can be found at:
http://www.jlr.org/content/suppl/2005/03/17/M400428-JLR200.DC1.html

TABLE 2. TC and EC mass in ARPE-19 and HepG2 cells

Sample	UC	EC	TC	EC as Percentage of TC
		μg/mg cell protein		
ARPE-19	21.35 ± 0.88	3.49 ± 0.58	24.83 ± 1.46	14.0%
HepG2	15.42 ± 0.72	14.63 ± 0.47	30.06 ± 1.19	48.7%

Data are representative of three independent experiments and are expressed as means ± SD. EC, esterified cholesterol; TC, total cholesterol; UC, unesterified cholesterol.

spectively), in contrast to control sections treated with the corresponding control immunoglobulins (Fig. 3B, D, respectively). Little apoB and MTP was detectable in unbleached sections (data not shown). To verify that this result was unrelated to the bleaching procedure, we examined immunoreactivity for MCT3, a basolaterally located, RPE-specific monocarboxylate transporter (37). Prior bleaching did not perturb the location of this antigen, and no intracellular granules were revealed (Fig. 3E, F). The coarse particulate labeling for apoB and MTP differed in size, shape, and distribution from both melanin granules (Fig. 3F) and autofluorescent lipofuscin granules (Fig. 3G). We conclude from these results that apoB and MTP are present in RPE, likely in the same subcellular compartment.

Expression of ACAT in retina and RPE

The above data support the hypothesis that EC-containing particles in human BrM could be particles with neutral lipid cores assembled and secreted by the RPE. To determine the capacity of RPE for esterifying cholesterol to long-chain fatty acids, we examined the expression of genes encoding ACAT-1 and ACAT-2, enzymes that catalyze cellular cholesterol esterification. In neurosensory retina, native RPE, ARPE-19, and HepG2, we detected the expected 413 bp RT-PCR products of ACAT-1 (**Fig. 4**). Despite our use of three different intron-spanning probes, the 494 bp RT-PCR product of ACAT-2 was detected only in HepG2 (Fig. 4).

Synthesis and secretion of neutral lipid-containing particles by ARPE-19

Because we found identical mRNA transcripts and apoB and MTP proteins in ARPE-19 cells as well as native RPE, we analyzed EC mass and composition in ARPE-19 cells. We compared the results with HepG2 cells, a widely used hepatocyte model system for apoB-containing lipoprotein secretion. **Table 2** shows that ARPE-19 contains EC, although at much lower absolute (3.5 μg/mg protein) and relative (14% of TC) levels than HepG2 (14.6 μg/mg and 48.7%, respectively). **Table 3** shows that by electrospray ionization mass spectrometry (ESI/MS), HepG2 contained 10- to 26-fold higher mass of cholesteryl palmitate, cholesteryl linoleate, cholesteryl oleate, and cholesteryl stearate than ARPE-19 and similar mass of cholesteryl arachidonate and cholesteryl docosahexanoate. Of these esters, both cell lines were relatively enriched in cholesteryl oleate, much more so in HepG2 than in ARPE-19.

To assess the ability of ARPE-19 cells to secrete EC, cells were incubated with serum-free medium containing oleic acid bound to BSA, and EC concentration in the conditioned medium was determined. In a series of three experiments, we detected 491 ± 35 μg/mg cell protein of TC, 234 ± 11 μg/mg cell protein of UC, and 257 ± 25 μg/mg cell protein of EC in conditioned medium. Thus, 52% of cholesterol recovered was esterified. In separate experiments, conditioned medium was subjected to density gradient ultracentrifugation. Esters were found only in the $d \leqslant 1.21$ g/ml fraction of conditioned medium and not in any fraction of nonconditioned medium (data not shown). **Table 4** shows that cholesteryl esters were detectable by ESI/MS in conditioned medium at levels 3- to 12-fold higher than in nonconditioned medium, depending on ester identity, with cholesteryl oleate most abundant.

To assess the de novo synthesis of lipids, ARPE-19 cells were metabolically labeled with [^{3}H]oleate-BSA and lipids were detected with TLC and scintillation counting. **Table 5** shows representative results from five independent experiments in which ARPE-19 cells were supplemented with radiolabeled oleic acid for 24 or 48 h. Radioactivity was high in bands corresponding to phospholipid, TG, and EC, relative to intervening bands. The medium contained more newly synthesized TG than EC at both time points. Twice as much radiolabeled TG and EC appeared in the medium after 48 h of incubation than after 24 h of incubation, consistent with sustained oleate uptake and conversion into TG and EC. In contrast, levels of newly synthesized phospholipid in the medium changed little during this time.

TABLE 3. Mass and composition of cholesteryl esters in ARPE-19 and HepG2 cells

Sample	Palmitate	Linoleate	Oleate	Stearate	Arachidonate	Docosahexanoate
			mass of cholesteryl ester (ng/mg cell protein)			
ARPE-19	49.34 ± 5.29	34.62 ± 4.72	87.17 ± 11.26	16.48 ± 2.02	37.83 ± 4.98	24.76 ± 4.96
HepG2	497.62 ± 19.55	256.89 ± 5.96	2,267.94 ± 108.90	265.59 ± 12.86	37.28 ± 0.92	37.51 ± 3.91
			% of cholesteryl esters measured			
ARPE-19	19.7%	13.8%	34.8%	6.6%	15.1%	9.9%
HepG2	14.8%	7.6%	67.4%	7.9%	1.1%	0.7%
			normalized to cholesteryl oleate			
ARPE-19	0.57 ± 0.01	0.40 ± 0.01	1.00	0.19 ± 0.00	0.43 ± 0.03	0.28 ± 0.02
HepG2	0.22 ± 0.01	0.11 ± 0.00	1.00	0.12 ± 0.00	0.016 ± 0.00	0.02 ± 0.00

Data are representative of three independent experiments performed in triplicate and are expressed as means ± SD.

Downloaded from www.jlr.org by guest, on June 14, 2012

Supplemental Material can be found at:
http://www.jlr.org/content/suppl/2005/03/17/M400428-JLR200.DC1.html

TABLE 4. Composition of cholesteryl esters in medium of oleate-BSA-supplemented ARPE-19

Variable	Palmitate	Linoleate	Oleate	Stearate	Arachidonate	Docosahexanoate
Mass (ng/mg cell protein)	69.75 ± 9.43	9.82 ± 1.97	26.39 ± 3.65	10.99 ± 0.62	11.90 ± 1.40	1.57 ± 0.18
Normalized	2.64	0.37	1.00	0.42	0.45	0.06
Fold increase over control	5.72	1.18	12.25	2.87	6.85	2.40

Data for mass and normalization are representative of three independent experiments performed in triplicate. All data were normalized to cholesteryl oleate. The fold increase in cholesteryl ester over nonconditioned medium represents the mean of three experiments.

To determine if EC in the d ⩽ 1.21 g/ml fraction of conditioned medium of oleate-supplemented ARPE-19 was associated with spherical particles, we used negative stain electron microscopy. Particles were detectable in medium (**Fig. 5A**) at a low abundance consistent with the low concentration of EC. For comparison, Fig. 5B shows plasma VLDL from a slightly hypertriglyceridemic subject at the same magnification. In contrast, particles were not detected in any fraction of nonconditioned medium.

ApoB/MTP expression and neutral lipid secretion by porcine RPE

Because the above experiments showed lipid secretion from a transformed cell line, we sought evidence that the apoB/MTP system was detectable in cultured primary RPE cells. The pig eye is advantageous for retina research, although it lacks a macula, because its large size and dual retinal vasculature resemble those of humans. To test whether porcine RPE and retina express mRNA for apoB and MTP, RT-PCR was performed, using porcine liver as a positive control. **Figure 6** shows that the expected RT-PCR products for apoB and MTP, 351 and 336 bp, respectively, were found. **Table 6** shows results representative of three metabolic labeling experiments using oleate-BSA and porcine RPE, demonstrating newly synthesized lipids in cells and medium at much higher levels (per microgram of cell protein) than in ARPE-19 (Table 5).

Localization of apoB and MTP in human neurosensory retina

The results presented to this point support our hypothesis regarding RPE, but Fig. 2 also indicates strong signals for apoB and MTP message and protein in neurosensory retina. To localize these proteins, cryosections of normal human macula were probed with polyclonal antibodies (**Fig. 7A**). Immunoreactivity was found in retinal ganglion cell (RGC) layer cells (Fig. 7B) and a few regularly spaced cells of the inner nuclear layer (INL; Fig. 7C). To determine the identity of these cells, double-label experiments were performed using a monoclonal antibody to Brn3a, a RGC marker (50) (Fig. 7D, E). All apoB-positive and MTP-positive cells in the RGC layer and INL were also Brn3a-positive. ApoB and MTP immunoreactivity formed large clumps within RGC perikarya and primary dendrites. We performed double-label immunofluorescence experiments using allophycocyanin- and FITC-tagged secondary antibodies to localize apoB and MTP, respectively. This experiment revealed that the same coarsely particulate clumps contained both antigens (Fig. 7F–H). In sections bleached to reveal RPE labeling (Fig. 3), RGC labeling was abolished (data not shown).

TABLE 5. New synthesis and secretion of phospholipid, TG, and EC by oleate-BSA-supplemented ARPE-19 cells

Sample	Phospholipid	TG	EC
		dpm/μg protein	
24 h cell	8,431 ± 527	9,728 ± 1,019	47 ± 4
48 h cell	10,889 ± 522	10,350 ± 405	105 ± 17
24 h medium	1,902 ± 80	217 ± 5	137 ± 10
48 h medium	2,258 ± 81	473 ± 26	367 ± 65

Data are representative of five independent experiments and are expressed as means ± SD. TG, triglyceride. Cells were incubated with 5 μCi/ml [^{3}H]oleate (5,000 dpm/nmol) bound to 1.5% fatty acid-free BSA.

DISCUSSION

The recognition that aging- and ARM-associated extracellular deposits contain apoB, apoE, and EC, and the presence of abundant EC-rich particles in normal human BrM, a vessel wall, underscore the potential role for lipoproteins in retinal health and disease, yet the lack of evidence for an association of ARM with increased plasma cholesterol is striking. Here, we demonstrate mRNA and protein for MTP in RPE and, unexpectedly, in RGC, providing a potential explanation for these findings. Immunohistochemical experiments suggest that apoB and MTP are colocalized in the same subcellular compartments within human RPE and RGC, presumably the endoplasmic reticulum. Stacks of rough endoplasmic reticulum typify long axon neurons, including RGC, but RPE has little rough and abundant smooth endoplasmic reticulum.

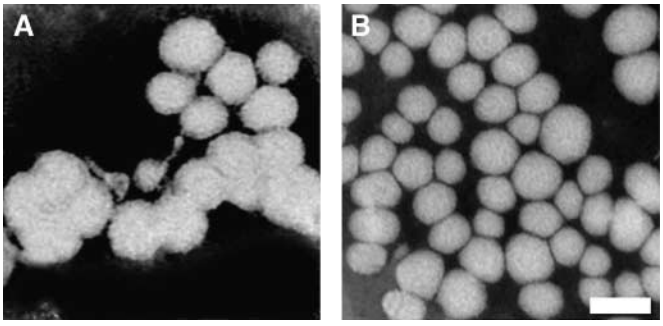

Fig. 5. Negative stain electron microscopy of lipoprotein-like particles. A: Particles resembling lipoproteins in the d ⩽ 1.21 g/ml fraction of medium conditioned by oleate-supplemented ARPE-19 cells. B: Human plasma VLDL. Bar = 50 nm.

Downloaded from www.jlr.org by guest, on June 14, 2012

Supplemental Material can be found at:
http://www.jlr.org/content/suppl/2005/03/17/M400428-JLR200.DC1.html

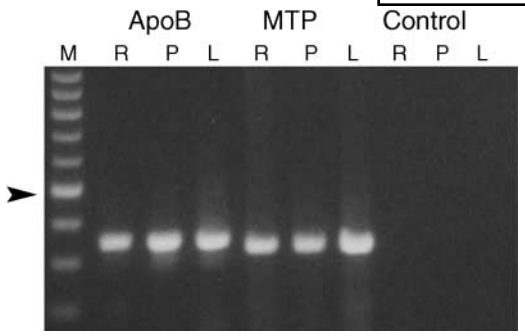

Fig. 6. Expression of apoB and MTP in porcine retina (R), RPE (P), and liver (L). Total RNA was isolated from porcine retina, RPE, and liver as described in Materials and Methods. Expected lengths of RT-PCR products are listed in Table 1. To check genomic DNA contamination, control reactions that lacked reverse transcriptase were performed for MTP. Primers for apoB span a 960 bp intron. M, 100 bp DNA ladder; arrowhead, 500 bp.

Confirming the exact identity of the subcellular compartment will require further experimentation.

In addition to MTP, we also detected mRNA transcripts for apoB, protein disulfide isomerase, and ACAT-1, but not APOBEC-1 or ACAT-2, in human retina, RPE, and ARPE-19. The complete transcriptome of retina- and RPE-expressed genes is a stated research goal (51), and the genes we report have not yet appeared in high-throughput surveys. Expression of essential RPE-specific genes is considered low relative to regulatory and housekeeping genes (52). However, MTP transcripts were reported for whole mouse eye (GenBank AV360595; H. Konno, K. Aizawa, S. Akahira et al., unpublished observations). We confirmed MTP mRNA and protein in murine retina/RPE (C-M. Li and X. Zhang, unpublished observations), in addition to our current result on porcine retina. MTP is the hallmark of cells that secrete lipoproteins with neutral lipid cores; therefore, we used metabolic labeling to ensure that neutral lipid synthesis and secretion by the ARPE-19 cell line and primary culture of porcine RPE were possible. Regarding ACAT, the ratio of ACAT proteins and mRNA transcripts differs among organs. By either measure, ACAT-1 predominates in liver and ACAT-2 predominates in intestine (53, 54). Retinal expression of ACAT-1 is consistent with the finding that ACAT-1 deficiency causes extensive UC deposition in brains of severely hypercholesterolemic mice (55). Expression of only one ACAT in a lipoprotein-secreting cell, if confirmed by other technologies, would be unusual.

TABLE 6. New synthesis and secretion of phospholipid, TG, and EC by oleate-BSA-supplemented porcine RPE cells

Sample	Phospholipid	TG	EC
		dpm/μg protein	
24 h cell	43,545 ± 8,000	3,666 ± 769	74,052 ± 11,380
48 h cell	23,177 ± 2,248	2,757 ± 669	72,470 ± 10,656
24 h medium	28,523 ± 4,571	1,438 ± 392	1,481 ± 379
48 h medium	73,023 ± 437	1,439 ± 232	650 ± 2

Data are representative of three independent experiments and are expressed as means ± SD. Cells were incubated with 5 μCi/ml [^{3}H]oleate (5,000 dpm/nmol) bound to 1.5% fatty acid-free BSA.

We detected apoB message and protein in native RPE. Intraocular mRNA transcripts for apoB were first detected for combined RPE/choroid (19) and then localized, with apoB protein, to native RPE (8). ApoB was detected in drusen by immunofluorescence (8) but not by proteomics (56), likely because the chloroform-methanol extraction used in that investigation removed core lipids and precipitated the amphipathic apoB peptide (57). In our report, ARPE-19 extracts contained a small but readily detectable high molecular mass band at the same position as in HepG2 extracts. We infer from its location, the sequencing of cDNA derived from apoB mRNA, and the lack of evidence for apoBEC-1 mRNA transcripts that this band represents apoB-100. We cannot exclude the possibility, however, that apoB-48, or another novel truncate, exists in the eye without using antibodies specific to apoB-48. However, because of the choice of cells, culture conditions, suboptimal lipid loading (see below), or inherently low secretion by RPE, we did not produce sufficient lipoprotein in culture medium to permit the extensive subfractionation for biochemical analysis of protein and lipid components that is possible for HepG2 (58, 59); thus, we were unable to demonstrate synthesis and secretion of apoB itself.

Despite the lack of secreted apoB, we did detect spherical lipid particles in the d ⩽ 1.21 g/ml fraction of medium conditioned by oleate-stimulated ARPE-19, supporting but not proving the idea that BrM particles are nascent lipoproteins. Particles were sparse, consistent with low EC concentration, and they were smaller than solid BrM particles in situ (12, 13), suggesting lower TG content. Although similar in size to plasma VLDL, ARPE-19-associated particles appeared more variable in diameter, possibly reflecting heterogeneity in FFA uptake or processing efficiency. Furthermore, differences in the amount of radiolabeled oleate incorporated into phospholipid at 24 and 48 h were minimal compared with those incorporated into TG and EC, suggesting that particle volumes after 48 h of incubation may be larger than particle volumes after 24 h, with proportionately smaller surface areas. Although ARPE-19-conditioned medium contained EC enriched in cholesteryl oleate and poor in cholesteryl docosahexanoate, BrM EC composition in vivo may differ, as the RPE regularly processes docosahexanoate-rich OS and BrM is exposed to plasma extravasated from the choroid. Notably, human RPE secretes apoE in vitro (21), 30% of which occurs in a fraction (d = 1.193–1.256 g/ml) that overlaps the EC-containing fraction of ARPE-19-conditioned medium. Thus, a potential setting for RPE apoE is the surface of a secreted apoB-containing lipoprotein (60). Finally, it is uncertain whether particles are secreted as such or form in the medium from secreted free apolipoproteins. For example, nascent apoA-I-containing high density lipoprotein particles that are discoidal and EC-poor [EC/TC, 0.16–0.22 (58, 61)] become spherical after acquiring EC in plasma via LCAT activity. Because native RPE and ARPE-19 express mRNA transcripts for LCAT (C-M.

Downloaded from www.jlr.org by guest, on June 14, 2012

Supplemental Material can be found at:
http://www.jlr.org/content/suppl/2005/03/17/M400428-JLR200.DC1.html

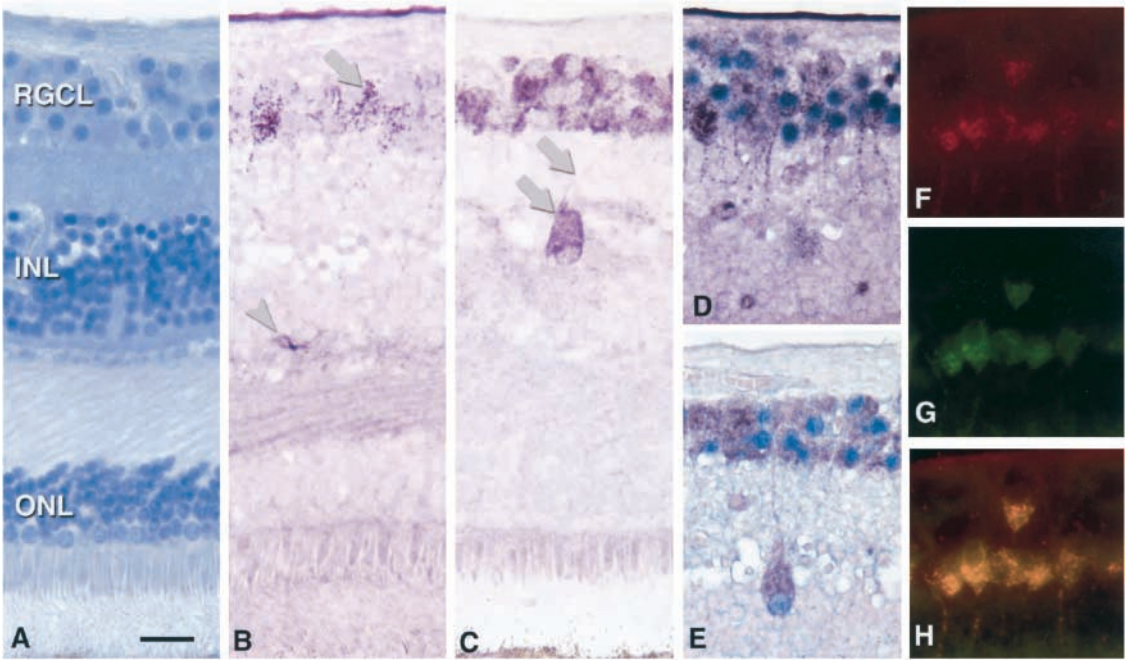

Fig. 7. Immunolocalization of apoB and MTP in neurosensory retina of normal human macula. Bar = 20 μm. A: Hematoxylin-stained retina. RGCL, retinal ganglion cell layer; INL, inner nuclear layer; ONL, outer nuclear layer. B: Goat anti-human apoB labels cell bodies and dendrites in RGCL (arrow) and plasma in capillaries (arrowhead). C: Rabbit anti-bovine MTP labels perikarya and dendrites in RGCL and INL (arrows). D, E: Double label for Brn3a (blue) and apoB (purple; D) or MTP (purple; E) confirms that apoB- and MTP-immunoreactive cells are RGC. F–H: Double-label immunofluorescence for apoB (allophycocyanin, red; F), MTP (FITC, green; G), and merged image (yellow; H) shows colocalization of these proteins in the same subcellular compartment.

Li, unpublished observations), similar metabolic remodeling may occur in culture. We think this unlikely, because the observed particles were EC-rich (EC/TC, 0.52) and spherical rather than discoidal. Furthermore, hepatic LCAT is believed to be active only in plasma. These uncertainties will be resolved using an improved culture system.

Determining the predominant FFA input to an RPE lipoprotein in vivo is an important goal for future study, with implications for retinal cell biology and ARM pathogenesis. The relative contributions of exogenous and de novo synthesized FFA to hepatic and intestinal lipoproteins are being actively investigated (62) using oleate-stimulated HepG2 cells. FFA delivery to neurosensory retina and RPE is best understood for docosahexanoate (63), preferentially enriched in neural membrane and photoreceptor OS phospholipids. The RPE is capable of both docosahexanoate biosynthesis (64) and LDL receptor-mediated apoB-containing lipoprotein uptake (65, 66). Thus, the relative contributions of exogenous and endogenous FFA to RPE secretory products must also be determined. However, the signature RPE lipid-processing activity is daily, light-synchronized phagocytosis of OS distal tips, so a potential source of exogenous FFA unique to RPE is phospholipids derived from these membrane-rich organelles. Our results with oleate-BSA indicate that phagocytosis is not required for neutral lipid secretion. However, lipoprotein assembly and secretion as a mechanism to release FFA from OS phospholipids as TG is an attractive hypothesis. Limited data on mammalian RPE support this notion, as intracellular TG in rat RPE cells increase for 4 h and decline over 24 h after OS phagocytosis in vivo (67) and in vitro (68). That OS phagocytosis, a uniquely eye-specific activity, should contribute lipids to ARM-associated lesions is a widely held expectation (69), but an output mechanism from RPE has never been specified. With an apoB-containing lipoprotein a plausible pathway for constitutive basolateral neutral lipid secretion, ARM lesion formation and its aftermath of inflammation and neovascularization can be reconceptualized as an atherosclerosis-like response-to-retention progression (26) with a local lipoprotein source. Testing this new hypothesis will be possible with an improved RPE culture system and animal models based on targeted deletion or overexpression of *MTP*.

Evidence for retinal *MTP* expression provides a basis to reexamine ABL from a novel perspective. ABL retinopathy involves macula and/or periphery and includes pigmentary changes, reduced electro-oculograms from RPE, reduced electroretinograms from cones and rods, predilection for angioid streaks (fractures in BrM) (70), and RPE cells with trilaminar inclusions in the subretinal space (71). For two decades, ABL retinopathy was attributed to systemic insufficiency of vitamin E transported by dietary apoB-containing lipoprotein (72). However, retinopathy persists or progresses despite vitamin E supplementation, even in patients treated from infancy to early adulthood (35, 71), and patients with undetectable plasma vitamin E can have normal retinas (73). Perhaps the clinical response to vitamin supplementation in ABL patients is variable, because *MTP* mutations directly cause a loss of

Downloaded from www.jlr.org by guest, on June 14, 2012

Supplemental Material can be found at:
http://www.jlr.org/content/suppl/2005/03/17/M400428-JLR200.DC1.html

function in retina. Furthermore, our unexpected finding of MTP and apoB in RGC, a neuron of the central nervous system, is potentially important for ABL neuropathy. Among retinal neurons, RGC is the most commonly affected in hereditary disorders of lipid metabolism (74). It is widely believed that the brain does not express apoB, and apoB-containing lipoproteins are undetectable in human cerebrospinal fluid (75). Unique among apolipoproteins, apoB is essential for brain development, and mice with absent or reduced apoB have neural tube defects (76, 77). Seeking *MTP* gene expression in brain with methods sensitive to low-abundance message is now warranted.

In summary, our results strengthen circumstantial evidence implicating apoB-containing lipoprotein assembly as an important retinal function, a plausible mechanism to place neutral lipid in BrM, and a candidate pathway involved in forming lipid-rich lesions in ARM. These data, along with the recently established cardiac apoB-containing lipoprotein (78), further widen the apoB/MTP system's role in mammalian physiology beyond classic functions of plasma TG transport.

The authors thank Drs. J. R. Wetterau and R. W. Milne for antibodies, N. J. Philp for a line of ARPE-19 and anti-MCT3, Ray Moore of the University of Alabama at Birmingham Mass Spectrometry Center for performing ESI/MS assays of cholesteryl esters, and the Alabama Eye Bank for timely retrieval of donor eyes. This work was supported by National Institutes of Health Grants EY-06109 (C.A.C.) and EY-13258 (C.G.), by the International Retinal Research Foundation, by unrestricted funds to the Department of Ophthalmology from Research to Prevent Blindness, Inc., by the EyeSight Foundation of Alabama, and by National Institutes of Health Grants P01 HL-34343 (N.D.), R01 HL-60936 (B.H.C.) and P30 CA-13148-32 to the University of Alabama at Birmingham Mass Spectrometry Center. C.A.C. received a Lew R. Wasserman Merit Award from Research to Prevent Blindness, Inc., and the 2002 Roger Johnson Prize in Macular Degeneration Research.

REFERENCES

1. Sarks, S. H. 1976. Ageing and degeneration in the macular region: a clinico-pathological study. *Br. J. Ophthalmol.* **60:** 324–341.
2. Green, W. R., and C. Enger. 1993. Age-related macular degeneration histopathologic studies: the 1992 Lorenz E. Zimmerman Lecture. *Ophthalmology.* **100:** 1519–1535.
3. Curcio, C. A., and C. L. Millican. 1999. Basal linear deposit and large drusen are specific for early age-related maculopathy. *Arch. Ophthalmol.* **117:** 329–339.
4. Pauleikhoff, D., S. Zuels, G. S. Sheraidah, J. Marshall, A. Wessing, and A. C. Bird. 1992. Correlation between biochemical composition and fluorescein binding of deposits in Bruch's membrane. *Ophthalmology.* **99:** 1548–1553.
5. Klaver, C. C., M. Kliffen, C. M. van Duijn, A. Hofman, M. Cruts, D. E. Grobbee, C. van Broeckhoven, and P. T. de Jong. 1998. Genetic association of apolipoprotein E with age-related macular degeneration. *Am. J. Hum. Genet.* **63:** 200–206.
6. Anderson, D. H., S. Ozaki, M. Nealon, J. Neitz, R. F. Mullins, G. S. Hageman, and L. V. Johnson. 2001. Local cellular sources of apolipoprotein E in the human retina and retinal pigmented epithelium: implications for the process of drusen formation. *Am. J. Ophthalmol.* **131:** 767–781.
7. Haimovici, R., D. L. Gantz, S. Rumelt, T. F. Freddo, and D. M. Small. 2001. The lipid composition of drusen, Bruch's membrane, and sclera by hot stage polarizing microscopy. *Invest. Ophthalmol. Vis. Sci.* **42:** 1592–1599.
8. Malek, G., C-M. Li, C. Guidry, N. E. Medeiros, and C. A. Curcio. 2003. Apolipoprotein B in cholesterol-containing drusen and basal deposits in eyes with age-related maculopathy. *Am. J. Pathol.* **162:** 413–425.
9. Klein, R., T. Peto, A. Bird, and M. R. Vannewkirk. 2004. The epidemiology of age-related macular degeneration. *Am. J. Ophthalmol.* **137:** 486–495.
10. Pauleikhoff, D., C. A. Harper, J. Marshall, and A. C. Bird. 1990. Aging changes in Bruch's membrane: a histochemical and morphological study. *Ophthalmology.* **97:** 171–178.
11. Holz, F. G., G. Sheraidah, D. Pauleikhoff, and A. C. Bird. 1994. Analysis of lipid deposits extracted from human macular and peripheral Bruch's membrane. *Arch. Ophthalmol.* **112:** 402–406.
12. Curcio, C. A., C. L. Millican, T. Bailey, and H. S. Kruth. 2001. Accumulation of cholesterol with age in human Bruch's membrane. *Invest. Ophthalmol. Vis. Sci.* **42:** 265–274.
13. Ruberti, J. W., C. A. Curcio, C. L. Millican, B. P. M. Menco, J-D. Huang, and M. Johnson. 2003. Quick-freeze/deep-etch visualization of age-related lipid accumulation in Bruch's membrane. *Invest. Ophthalmol. Vis. Sci.* **44:** 1753–1759.
14. Curcio, C. A., J. B. Presley, C. L. Millican, and N. E. Medeiros. 2005. Basal deposits and drusen in eyes with age-related maculopathy: evidence for solid lipid particles. *Exp. Eye Res.* In press.
15. Sheraidah, G., R. Steinmetz, J. Maguire, D. Pauleikhoff, J. Marshall, and A. C. Bird. 1993. Correlation between lipids extracted from Bruch's membrane and age. *Ophthalmology.* **100:** 47–51.
16. Nguyen-Legros, J., and D. Hicks. 2000. Renewal of photoreceptor outer segments and their phagocytosis by the retinal pigment epithelium. *Int. Rev. Cytol.* **196:** 245–313.
17. Campochiaro, P. A., J. A. Jerdan, and B. M. Glaser. 1986. The extracellular matrix of human retinal pigment epithelial cells in vivo and its synthesis in vitro. *Invest. Ophthalmol. Vis. Sci.* **27:** 1615–1621.
18. Hewitt, T. A., K. Nakasawa, and D. A. Newsome. 1989. Analysis of newly synthesized Bruch's membrane proteoglycans. *Invest. Ophthalmol. Vis. Sci.* **30:** 478–486.
19. Mullins, R. F., S. R. Russell, D. H. Anderson, and G. S. Hageman. 2000. Drusen associated with aging and age-related macular degeneration contain proteins common to extracellular deposits associated with atherosclerosis, elastosis, amyloidosis, and dense deposit disease. *FASEB J.* **14:** 835–846.
20. Hageman, G. S., P. J. Luthert, N. H. C. Chong, L. V. Johnson, D. H. Anderson, and R. F. Mullins. 2001. An integrated hypothesis that considers drusen as biomarkers of immune-mediated processes at the RPE-Bruch's membrane interface in aging and age-related macular degeneration. *Prog. Retin. Eye Res.* **20:** 705–732.
21. Ishida, B. Y., K. R. Bailey, K. G. Duncan, R. J. Chalkley, A. L. Burlingame, J. P. Kane, and D. M. Schwartz. 2004. Regulated expression of apolipoprotein E by human retinal pigment epithelial cells. *J. Lipid Res.* **45:** 263–271.
22. Smith, W., J. Assink, R. Klein, P. Mitchell, C. C. W. Klaver, B. E. K. Klein, A. Hofman, S. Jensen, J. J. Wang, and P. T. V. M. de Jong. 2001. Risk factors for age-related macular degeneration. Pooled findings from three continents. *Ophthalmology.* **108:** 697–704.
23. Age-Related Eye Disease Study Group. 2000. Risk factors associated with age-related macular degeneration. A case-control study in the Age-Related Eye Disease Study: Age-Related Eye Disease Study Report Number 3. *Ophthalmology* **107:** 2224–2232.
24. Eye Disease Case-Control Study Group. 1992. Risk factors for neovascular age-related macular degeneration. *Arch. Ophthalmol.* **110:** 1701–1708.
25. Verschuren, W. M., D. R. Jacobs, B. P. Bloemberg, D. Kromhout, A. Menotti, C. Aravanis, H. Blackburn, R. Buzina, A. S. Dontas, F. Fidanza, et al. 1995. Serum total cholesterol and long-term coronary heart disease mortality in different cultures. Twenty-five-year follow-up of the seven countries study. *J. Am. Med. Assoc.* **274:** 131–136.
26. Williams, K. J., and I. Tabas. 1995. The response-to-retention hypothesis of early atherogenesis. *Arterioscler. Thromb. Vasc. Biol.* **15:** 551–561.
27. Kruth, H. S. 1997. Cholesterol deposition in atherosclerotic lesions. *Subcell. Biochem.* **28:** 319–362.
28. Smith, E. 1973. Relationship between plasma lipids and arterial tissue lipids. *Nutr. Metab.* **15:** 17–26.

Downloaded from www.jlr.org by guest, on June 14, 2012

Supplemental Material can be found at:
http://www.jlr.org/content/suppl/2005/03/17/M400428-JLR200.DC1.html

29. Wetterau, J. R., M. C. Lin, and H. Jamil. 1997. Microsomal triglyceride transfer protein. *Biochim. Biophys. Acta.* **1345:** 136–150.
30. Gordon, D. A., and H. Jamil. 2000. Progress towards understanding the role of microsomal triglyceride transfer protein in apolipoprotein-B lipoprotein assembly. *Biochim. Biophys. Acta.* **1486:** 72–83.
31. Wetterau, J. R., L. P. Aggerbeck, M. E. Bouma, C. Eisenberg, A. Munck, M. Hermier, J. Schmitz, G. Gay, D. J. Rader, and R. E. Gregg. 1992. Absence of microsomal triglyceride transfer protein in individuals with abetalipoproteinemia. *Science.* **258:** 999–1001.
32. Gordon, D. A., H. Jamil, D. Sharp, D. Mullaney, Z. Yao, R. E. Gregg, and J. Wetterau. 1994. Secretion of apolipoprotein B-containing lipoproteins from HeLa cells is dependent on expression of the microsomal triglyceride transfer protein and is regulated by lipid availability. *Proc. Natl. Acad. Sci. USA.* **91:** 7628–7632.
33. Leiper, J. M., J. D. Bayliss, R. J. Pease, D. J. Brett, J. Scott, and C. C. Shoulders. 1994. Microsomal triglyceride transfer protein, the abetalipoproteinemia gene product, mediates the secretion of apolipoprotein B-containing lipoproteins from heterologous cells. *J. Biol. Chem.* **269:** 21951–21954.
34. Sellers, J. A., and G. S. Shelness. 2001. Lipoprotein assembly capacity of the mammary tumor-derived cell line C127 is due to the expression of functional microsomal triglyceride transfer protein. *J. Lipid Res.* **42:** 1897–1904.
35. Berriot-Varoqueaux, N., L. P. Aggerbeck, M. Samson-Bouma, and J. R. Wetterau. 2000. The role of the microsomal triglyceride transfer protein in abetalipoproteinemia. *Annu. Rev. Nutr.* **20:** 663–697.
36. Dunn, K. C., A. E. Aotaki-Keen, F. R. Putkey, and L. M. Hjelmeland. 1996. ARPE-19, a human retinal pigment epithelial cell line with differentiated properties. *Exp. Eye Res.* **62:** 155–162.
37. Philp, N. J., D. Wang, H. Yoon, and L. M. Hjelmeland. 2003. Polarized expression of monocarboxylate transporters in human retinal pigment epithelium and ARPE-19 cells. *Invest. Ophthalmol. Vis. Sci.* **44:** 1716–1721.
38. Blackburn, J., E. E. Tarttelin, C. Y. Gregory-Evans, M. Moosajee, and K. Gregory-Evans. 2003. Transcriptional regulation and expression of the dominant drusen gene FBLN3 (EFEMP1) in mammalian retina. *Invest. Ophthalmol. Vis. Sci.* **44:** 4613–4621.
39. Mamballikalathil, I., C. Mann, and C. Guidry. 2000. Tractional force generation by porcine Müller cells: stimulation by retinal pigment epithelial cell-secreted growth factor. *Invest. Ophthalmol. Vis. Sci.* **41:** 529–536.
40. Levy, E., S. Stan, E. Delvin, D. Menard, C. Shoulders, C. Garofalo, I. Slight, E. Seidman, G. Mayer, and M. Bendayan. 2002. Localization of microsomal triglyceride transfer protein in the Golgi. Possible role in the assembly of chylomicrons. *J. Biol. Chem.* **277:** 16470–16477.
41. Wang, X., R. Bucala, and R. Milne. 1998. Epitopes close to the apolipoprotein B low density lipoprotein receptor-binding site are modified by advanced glycation end products. *Proc. Natl. Acad. Sci. USA.* **95:** 7643–7647.
42. Bhutto, I. A., S. Y. Kim, D. S. McLeod, C. Merges, N. Fukai, B. R. Olsen, and G. A. Lutty. 2004. Localization of collagen XVIII and the endostatin portion of collagen XVIII in aged human control eyes and eyes with age-related macular degeneration. *Invest. Ophthalmol. Vis. Sci.* **45:** 1544–1552.
43. Li, C-M., R. T. Yan, and S-Z. Wang. 2002. Chick homeobox gene cbx and its role in retinal development. *Mech. Dev.* **116:** 85–94.
44. Folch, P., M. Lees, and G. H. Sloane-Stanley. 1957. A simple method for the purification of total lipids from animal tissues. *J. Biol. Chem.* **226:** 497–509.
45. Gamble, W., M. Vaughan, H. S. Kruth, and T. Avigan. 1978. Procedure for determination of free and total cholesterol in micro- or nanogram amounts suitable for studies with cultured cells. *J. Lipid Res.* **19:** 1068–1070.
46. Dixon, J. L., S. Furukawa, and H. N. Ginsberg. 1991. Oleate stimulates secretion of apolipoprotein B-containing lipoproteins from Hep G2 cells by inhibiting early intracellular degradation of apolipoprotein B. *J. Biol. Chem.* **266:** 5080–5086.
47. Forte, T. M., and R. W. Nordhausen. 1986. Electron microscopy of negatively stained lipoproteins. *Methods Enzymol.* **128:** 442–457.
48. Davidson, N. O., and G. S. Shelness. 2000. Apolipoprotein B: mRNA editing, lipoprotein assembly, and presecretory degradation. *Annu. Rev. Nutr.* **20:** 169–193.
49. Foss, A. J., R. A. Alexander, L. W. Jefferies, and S. Lightman. 1995. Immunohistochemical techniques: the effect of melanin bleaching. *Br. J. Biomed. Sci.* **52:** 22–25.
50. Liu, W., S. L. Khare, X. Liang, M. A. Peters, X. Liu, C. L. Cepko, and M. Xiang. 2000. All Brn3 genes can promote retinal ganglion cell differentiation in the chick. *Development.* **127:** 3237–3247.
51. Swaroop, A., and D. J. Zack. 2002. Transcriptome analysis of the retina. *Genome Biol.* **3:** 1022.1021–1022.1024.
52. Sharon, D., S. Blackshaw, C. L. Cepko, and T. P. Dryja. 2002. Profile of the genes expressed in the human peripheral retina, macula, and retinal pigment epithelium determined through serial analysis of gene expression (SAGE). *Proc. Natl. Acad. Sci. USA.* **99:** 315–320.
53. Chang, C. C., N. Sakashita, K. Ornvold, O. Lee, E. T. Chang, R. Dong, S. Lin, C. Y. Lee, S. C. Strom, R. Kashyap, J. J. Fung, R. V. Farese, Jr., J. F. Patoiseau, A. Delhon, and T. Y. Chang. 2000. Immunological quantitation and localization of ACAT-1 and ACAT-2 in human liver and small intestine. *J. Biol. Chem.* **275:** 28083–28092.
54. Smith, J. L., K. Rangaraj, R. Simpson, D. J. Maclean, L. K. Nathanson, K. A. Stuart, S. P. Scott, G. A. Ramm, and J. de Jersey. 2004. Quantitative analysis of the expression of ACAT genes in human tissues by real-time PCR. *J. Lipid Res.* **45:** 686–696.
55. Accad, M., S. J. Smith, D. L. Newland, D. A. Sanan, L. E. King, Jr., M. F. Linton, S. Fazio, and R. V. Farese, Jr. 2000. Massive xanthomatosis and altered composition of atherosclerotic lesions in hyperlipidemic mice lacking acyl CoA:cholesterol acyltransferase 1. *J. Clin. Invest.* **105:** 711–719.
56. Crabb, J. W., M. Miyagi, X. Gu, K. Shadrach, K. A. West, H. Sakaguchi, M. Kamei, A. Hasan, L. Yan, M. E. Rayborn, R. G. Salomon, and J. G. Hollyfield. 2002. Drusen proteome analysis: an approach to the etiology of age-related macular degeneration. *Proc. Natl. Acad. Sci. USA.* **99:** 14682–14687.
57. Fisher, W. R., and V. N. Schumaker. 1986. Isolation and characterization of apolipoprotein B-100. *Methods Enzymol.* **128:** 247–262.
58. Thrift, R. N., T. M. Forte, B. E. Cahoon, and V. G. Shore. 1986. Characterization of lipoproteins produced by the human liver cell line, Hep G2, under defined conditions. *J. Lipid Res.* **27:** 236–250.
59. Dashti, N. 1991. Synthesis and secretion of nascent lipoprotein particles. *Prog. Lipid Res.* **30:** 219–230.
60. Swift, L. L., P. D. Soule, and V. S. LeQuire. 1982. Hepatic Golgi lipoproteins: precursors to plasma lipoproteins in hypercholesterolemic rats. *J. Lipid Res.* **23:** 962–971.
61. Johnson, F. L., J. Babiak, and L. L. Rudel. 1986. High density lipoprotein accumulation in perfusates of isolated livers of African green monkeys. Effects of saturated versus polyunsaturated dietary fat. *J. Lipid Res.* **27:** 537–548.
62. Zhang, Y-L., A. Hernandez-Ono, C. Ko, K. Yasanuga, L-S. Huang, and H. N. Ginsberg. 2004. Regulation of hepatic apolipoprotein-B lipoprotein assembly and secretion by the availability of fatty acids. I. Differential response to the delivery of fatty acids via albumin or remnant-like emulsion particles. *J. Biol. Chem.* **279:** 19362–19374.
63. Bazan, N. G., W. C. Gordon, and E. B. Rodriguez de Turco. 1992. Docosahexaenoic acid uptake and metabolism in photoreceptors: retinal conservation by an efficient retinal pigment epithelial cell-mediated recycling process. *Adv. Exp. Med. Biol.* **318:** 295–306.
64. Wang, N., and R. E. Anderson. 1993. Synthesis of docosahexaenoic acid by retina and retinal pigment epithelium. *Biochemistry.* **32:** 13703–13709.
65. Hayes, K. C., S. Lindsey, Z. F. Stephan, and D. Brecker. 1989. Retinal pigment epithelium possesses both LDL and scavenger receptor activity. *Invest. Ophthalmol. Vis. Sci.* **30:** 225–232.
66. Elner, V. M. 2002. Retinal pigment epithelial acid lipase activity and lipoprotein receptors: effects of dietary omega-3 fatty acids. *Trans. Am. Ophthalmol. Soc.* **100:** 301–338.
67. Baker, B., M. Moriya, M. Maude, R. Anderson, and T. Williams. 1986. Oil droplets of the retinal epithelium of the rat. *Exp. Eye Res.* **42:** 547–557.
68. Rodriguez de Turco, E. B., N. Parkins, A. V. Ershov, and N. G. Bazan. 1999. Selective retinal pigment epithelial cell lipid metabolism and remodeling conserves photoreceptor docosahexaenoic acid following phagocytosis. *J. Neurosci. Res.* **57:** 479–486.
69. Young, R. W. 1987. Pathophysiology of age-related macular degeneration. *Surv. Ophthalmol.* **31:** 291–306.
70. Gorin, M. B., T. O. Paul, and D. J. Rader. 1994. Angioid streaks associated with abetalipoproteinemia. *Ophthalmic Genet.* **15:** 151–159.
71. Chowers, I., E. Banin, S. Merin, M. Cooper, and E. Granot. 2001. Long-term assessment of combined vitamin A and E treatment for the prevention of retinal degeneration in abetalipoproteinaemia and hypobetalipoproteinaemia patients. *Eye.* **15:** 525–530.
72. Runge, P., D. P. Muller, J. McAllister, D. Calver, J. K. Lloyd, and D.

Downloaded from www.jlr.org by guest, on June 14, 2012

Supplemental Material can be found at:
http://www.jlr.org/content/suppl/2005/03/17/M400428-JLR200.DC1.html

Taylor. 1986. Oral vitamin E supplements can prevent the retinopathy of abetalipoproteinaemia. *Br. J. Ophthalmol.* **70:** 166–173.
73. Al-Shali, K., J. Wang, F. Rosen, and R. Hegele. 2003. Ileal adenocarcinoma in a mild phenotype of abetalipoproteinemia. *Clin. Genet.* **63:** 135–138.
74. Levin, L., and L. Gordon. 2002. Retinal ganglion cell disorders: types and treatments. *Prog. Retin. Eye Res.* **21:** 465–484.
75. Koch, S., N. Donarski, K. Goetze, M. Kreckel, H-J. Stuerenburg, C. Buhmann, and U. Beisiegel. 2001. Characterization of four lipoprotein classes in human cerebrospinal fluid. *J. Lipid Res.* **42:** 1143–1151.
76. Farese, R. V., Jr., S. L. Ruland, L. M. Flynn, R. P. Stokowski, and S. G. Young. 1995. Knockout of the mouse apolipoprotein B gene results in embryonic lethality in homozygotes and protection against diet-induced hypercholesterolemia in heterozygotes. *Proc. Natl. Acad. Sci. USA.* **92:** 1774–1778.
77. Raabe, M., L. M. Flynn, C. H. Zlot, J. S. Wong, M. M. Veniant, R. L. Hamilton, and S. G. Young. 1998. Knockout of the abetalipoproteinemia gene in mice: reduced lipoprotein secretion in heterozygotes and embryonic lethality in homozygotes. *Proc. Natl. Acad. Sci. USA.* **95:** 8686–8691.
78. Björkegren, J., M. Veniant, S. K. Kim, S. K. Withycombe, P. A. Wood, M. K. Hellerstein, R. A. Neese, and S. G. Young. 2001. Lipoprotein secretion and triglyceride stores in the heart. *J. Biol. Chem.* **276:** 38511–38517.
79. Lu, S., M. Huffman, Y. Yao, C. M. Mansbach, 2nd, X. Cheng, S. Meng, and D. D. Black. 2002. Regulation of MTP expression in developing swine. *J. Lipid Res.* **43:** 1303–1311.

ASBMB JOURNAL OF LIPID RESEARCH JLR

Downloaded from www.jlr.org by guest, on June 14, 2012